Supporting Information

Ma et al. 10.1073/pnas.0810300106

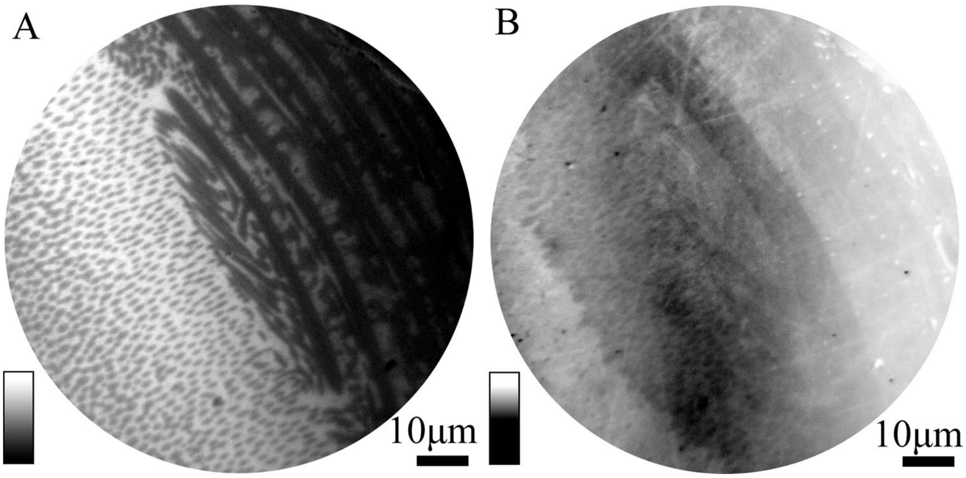

Fig. S1. (*A* and *B*) Mg distribution (*A*) and oxygen PIC (*B*) maps from the center of the stone part show the morphology (*A*) and orientation (gray levels in *B*) of the single crystalline needles, plates and polycrystalline matrix.

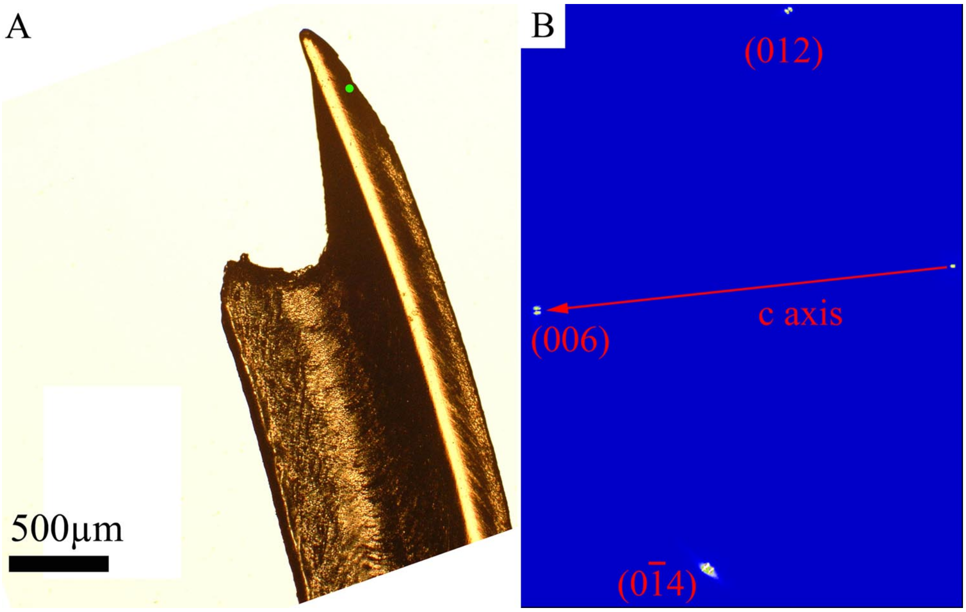

Fig. S2. A longitudinal thin section of the grinding tip of the sea urchin tooth (*A*) and the microbeam x-ray diffraction pattern (*B*) obtained from the position with the green dot in *A*. The diffraction pattern was taken at a rotation angle of 7.5°, with an oscillation angle ± 2.5°. The zone axis of calcite in the diffraction pattern is [100]. The *c*-axes of calcite are -6° from the horizontal direction (*B*) and the tooth growth direction is 69° from the horizontal direction according to the bright line (the stone part in *A*). Therefore the *c*-axes of calcite are about 75° from the growth direction of the tooth. The (006) reflection splits into two strong reflections, which differ by 0.6° in azimuthal direction.

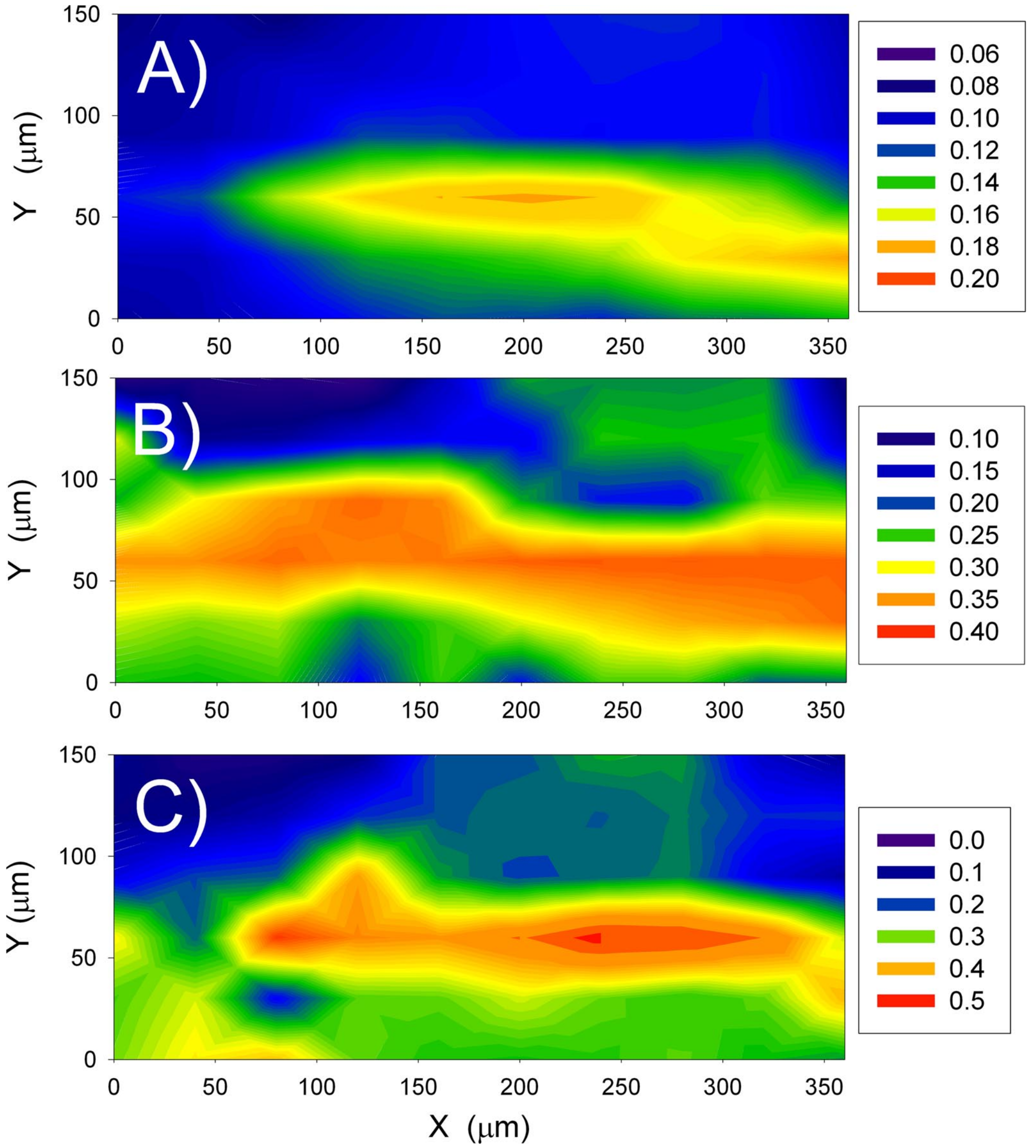

Fig. S3. Map of chemical and compositional parameters in the sea urchin tooth in the transverse cross-section obtained from the analysis of microbeam x-ray diffraction patterns within the box in Fig. 2*A*. (*A* and *B*) Maps of the Mg contents (atomic percent, Mg% + Ca% = 100%) in the plates/needles (x_1) (*A*) and in the polycrystalline matrix (x_2) (*B*). The quantitative values for the Mg content shown by a pseudocolor scale are indicated on the right hand side of the images. (*C*) Map of the relative amount of polycrystalline matrix (ϕ), with the quantitative values for the pseudocolor scale again indicated. (*A–C*) Images created from the mesh-scan within the box in Fig. 2*A*. The mean Mg content for the needle/plate complex and the polycrystalline matrix was calculated from the (104) peak positions (see Fig. 3) using the known dependence of the calcite lattice parameters *a* and *c* on Mg content [Hellwege K-H, Hellwege AM eds (1979) *Crystal Structure Data of Inorganic Compounds*. Landolt Börnstein, New Series (Springer, Berlin) Vol 3, Group 7, pp 105]. This was performed by creating a linear calibration curve $x = k_{1q104} + k_2$, using $q_{104} = 2\pi\sqrt{(4/3a2) + 16/c^2}$ with $k_1 = 2.1854$ and $k_2 = 20.6463$ nm. Here, *x* is the Mg content and q_{104} the radial position of the corresponding Bragg peak, the length of the scattering vector *q* being defined as $q = 4\pi\sin(\theta)/\lambda$ (2θ and λ are the scattering angle and the wavelength, respectively). *A* and *B* show a clear gradient of the mean Mg content for the needles/plates and the polycrystalline matrix respectively, in the vertical direction. The highest amount of Mg for each structural component is observed in a roughly horizontal stripe across the grinding tip, indicating that the mean Mg content increases strongly in the stone part as compared to the neighboring regions. The absolute value of about 40% Mg content of the polycrystalline matrix in the stone part agrees well with the value obtained from Nano-SIMS. There is a large difference in Mg contents between the plate/needle complex and the polycrystalline matrix (note the different scales in *A* and *B*). Interestingly, this difference is largest in the stone part, indicating a spatially varying ''chemical contrast'' between the two structural elements (difference image not shown). The third image (Fig. 3*C*) shows the relative amount $\phi = I_2/(I_1 + I_2)$ of polycrystalline matrix, where I_1 and I_2 are the intensities of the left and the right peak in Fig. 3, respectively. It constitutes therefore a composition contrast between the two phases. This image shows clearly that the amount of polycrystalline matrix is also highest in the stone part (about 50%), and is higher at the bottom needle-rich region (about 30%) as compared to the top plate-rich region (10–20%).

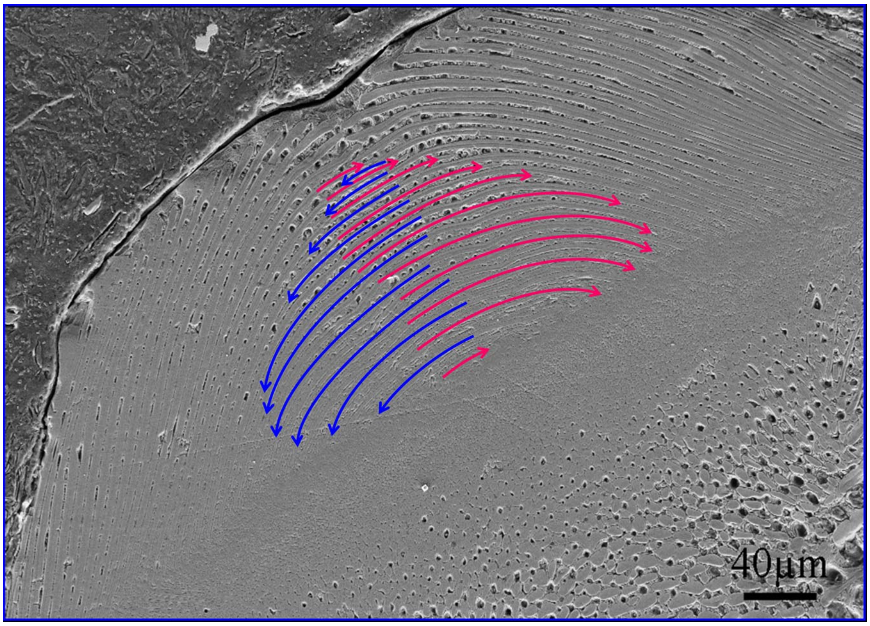

Fig. S4. SEM image of a transverse cross-section of a sea urchin tooth at the mature end (grinding tip), and the stone part at its center. The blue arrows show the extensions of the primary plates from the right side and the magenta arrows show the extensions of the primary plates from the left side.

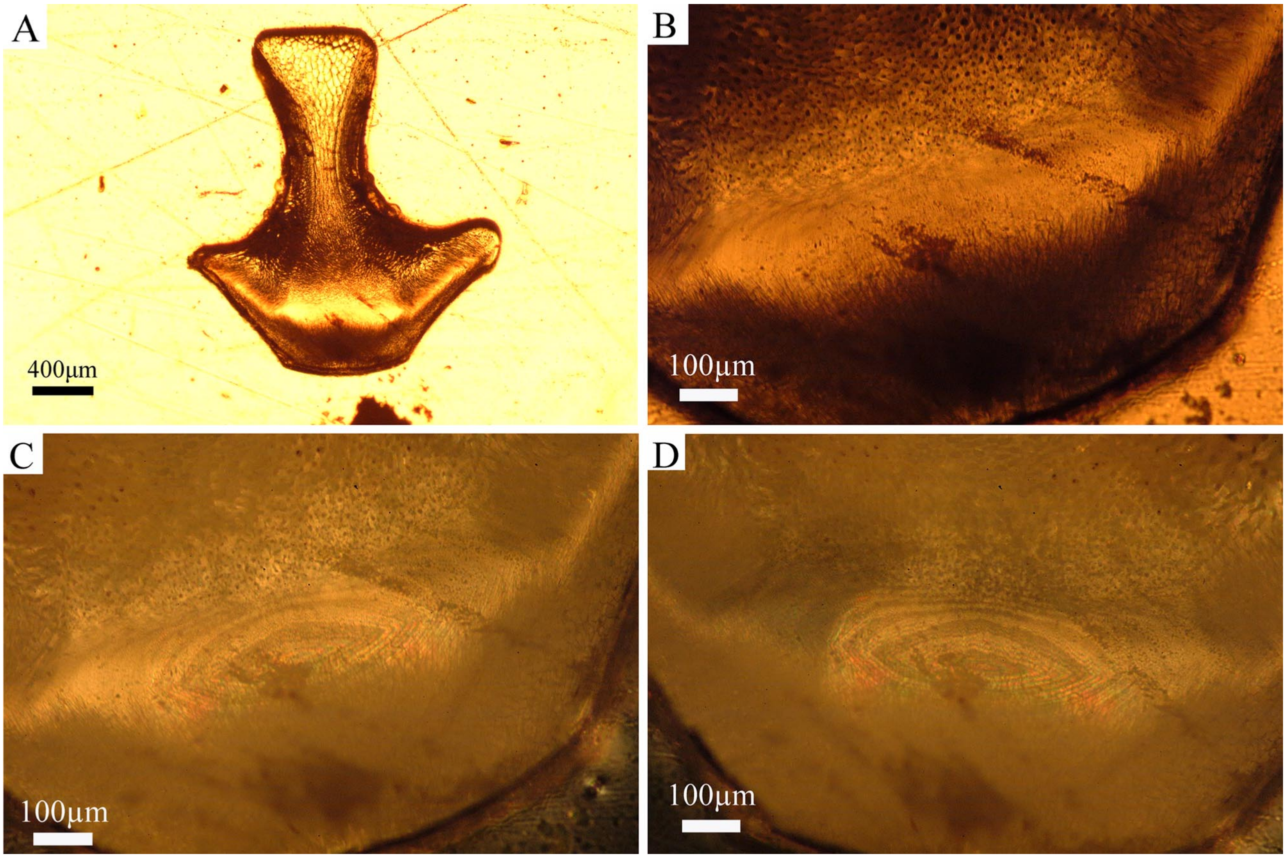

Fig. S5. Light microscopy images of the mature tooth cross-section with thickness 170 μm under plain (*A* and *B*) and polarized light (*C* and *D*). The sample in *D* was rotated clockwise by 20° from its position in *C*. Ring-like structures appear at the center of the stone part with alternate bright or dark traces. (*C*) The bright center became dark when the sample was rotated clockwise by 20° (compare *C* with *D*). As in PIC maps, polarized light images indicate two alternating crystal orientations in the stone part of the tooth. However, no quantitative information about the two crystal orientations could be obtained from the polarized light microscopy images.